# Temporal dynamics of nitrogen cycle gene diversity in a hyporheic microbiome

William C. Nelson[1]* (william.nelson@pnnl.gov), Emily B. Graham[1] (emily.graham@pnnl.gov), Alex R. Crump[2] (acrump@uidaho.edu), Sarah J. Fansler[1] (sarah.fansler@pnnl.gov), Evan V. Arntzen[1] (evan.arntzen@pnnl.gov), David W. Kennedy[1] (dwkennedy61@gmail.com), and James C. Stegen[1] (james.stegen@pnnl.gov)

[1] Pacific Northwest National Laboratory, Richland, WA, U.S.A

[2] Department of Soil and Water Systems, University of Idaho, Moscow, ID, U.S.A.

*Corresponding author.

William C. Nelson

PO Box 999, MSIN J4-18

Richland, WA 99352

Phone: (509)375-4442

FAX: 509-375-1368

Email: william.nelson@pnnl.gov

Running head: Gene-level diversity in microbial systems

Keywords: microbial ecology; community function; genetic diversity; denitrification; nitrification

## ABSTRACT

Biodiversity is thought to prevent decline in community function in response to changing environmental conditions through replacement of organisms with similar functional capacity but different optimal growth characteristics. We examined how this concept translates to the within-gene level by exploring seasonal dynamics of within-gene diversity for genes involved in nitrogen cycling in hyporheic zone communities. Nitrification genes displayed low richness—defined as the number of unique within-gene phylotypes—across seasons. Conversely, denitrification genes varied in both richness and the degree to which phylotypes were recruited or lost. These results demonstrate that there is not a universal mechanism for maintaining community functional potential for nitrogen cycling activities, even across seasonal environmental shifts to which communities would be expected to be well adapted. As such, extreme environmental changes could have very different effects on the stability of the different nitrogen cycle activities. These outcomes suggest a need to modify existing conceptual models that link biodiversity to microbiome function to incorporate within-gene diversity. Specifically, we suggest an expanded conceptualization that (1) recognizes component steps (genes) with low diversity as potential bottlenecks influencing pathway-level function, and (2) includes variation in both the number of entities (*e.g.* species, phylotypes) that can contribute to a given process and the turnover of those entities in response to shifting conditions. Building these concepts into process-based ecosystem models represents an exciting opportunity to connect within-gene-scale ecological dynamics to ecosystem-scale services.

## INTRODUCTION

High microbial diversity has been observed in almost all environments that have been examined (Gibbons and Gilbert 2015). It is widely believed that this diversity provides functional stability to ecosystems experiencing fluctuations in environmental conditions by the presence of organisms having overlapping functional capabilities but different conditions under which they optimally function (Allison and Martiny 2008; Hooper et al. 2005; Rosenfeld 2002; Shade et al. 2012; Torsvik and Ovreas 2002; Walker 1992; Yachi and Loreau 1999). In a fluctuating environment, conditions that impair the growth of some populations will stimulate the growth of others, and overall community function is maintained. Maintenance of higher diversity therefore allows a community to respond more rapidly to a disturbance or environmental shift and reduces its dependence on (or susceptibility to) recruitment of new organisms to fill vacant niches. The dynamics of diversity at the functional gene level, however, have not been well explored.

Cooperative metabolism in natural microbial communities has long been suspected, but only recently have metagenomic studies revealed its extent. The component steps of complex metabolic pathways, such as denitrification, sulfur oxidation, and organic carbon degradation, have been observed to be distributed across multiple organisms more frequently than they are co-resident in a single organism (Anantharaman et al. 2016; Mobberley et al. 2017). Distributed metabolism likely reflects efficiency gains from specialization and division of labor (West and Cooper 2016). This partitioning, however, puts component steps of critical ecosystem processes under different selective pressures, according to which organism encodes them. Temporal dynamics of diversity and abundance may, therefore, vary significantly across component steps.

Nitrogen cycling is an excellent and ubiquitous example of a complex, distributed process. While complete denitrifier organisms, such as *Pseudomonas aeruginosa* and *Parcoccus denitrificans*,

have been isolated and described, it has long been suspected that many organisms encode partial pathways and can act in concert to cycle nitrogen between its reduced and oxidized forms (Zumft 1997). More recently, genome sequence data from both isolates and environmental samples has shown that many organisms encode various subsets of denitrification activities (Anantharaman et al. 2016; Graf et al. 2014). Several previous studies have investigated the abundance and distribution of nitrogen cycling activities in environmental microbiomes (Bru et al. 2011; Graham et al. 2014; Keil et al. 2011; Nelson et al. 2015; Nelson et al. 2016; Stoliker et al. 2016), none yet have specifically tracked the diversity of individual gene families that comprise nitrogen transformation pathways across fluctuating environmental conditions.

Here we take advantage of seasonal shifts in hydrology and aqueous geochemistry within a hyporheic zone system that have been shown to alter microbial community structure (Graham et al. 2016a; Graham et al. 2017), and examine the temporal dynamics of diversity within major N-cycling genes encoding steps in nitrification and denitrification. Some component steps consistently showed very low diversity, while others displayed significant temporal variation in the level of diversity and turnover in the contributing phylotypes across divergent environmental conditions. The observed heterogeneity through time and across component steps indicates that predictive ecosystem models that explicitly represent microbial communities should account for variation in and dynamics of within-gene diversity of component steps of key processes.

## RESULTS

*Seasonal environmental changes.* Sediment communities from the hyporheic zone of the Columbia River along the Hanford Reach were sampled from April 30, 2014 to November 25, 2014, using sand packs deployed at three locations (T2, T3, and T4) for six weeks at a time (Graham et al. 2016b). Water chemistry data taken in parallel at the three sites showed similar,

yet not identical temporal patterns. A mid-year shift in hydraulic regime was observed, with higher influx of surface water in the spring resulting in higher levels of dissolved organic carbon (measured as non-purgeable organic carbon) (NPOC) (0.8-1.0 mg/L) (**Fig 1A**) and low levels of nitrate (10-15 µM) (**Fig 1B**), transitioning to a more groundwater-influenced condition in the fall, increasing the nitrate concentrations (up to 300 µM) and decreasing NPOC concentration (down to <0.4 mg/L). Because the groundwater in this system is oxic, the DO concentration was fairly constant for the duration of sampling, ranging from ~60-100% saturation (**Fig 1C**). The water temperature followed expected seasonal trends, warming in the summer and cooling in the fall (**Fig 1D**). Sampling times were categorized as early (Apr 30 through Jul 22) or late (Sep 2 through Nov 30), based on these observations.

*Organism-level diversity.* Organismal diversity was measured by 16S rRNA amplicon sequence analysis and extraction and assembly of *rplB* gene sequences from the metagenomic data sets (**Fig 2**). As reported previously (Graham et al. 2016a), species richness correlated best with water temperature. Diversity, as measured by the inverse Simpson statistic, was high and mirrored species richness, suggesting high evenness. Two late samples, October 14 and November 25, showed high richness but low diversity, driven by a bloom of Bacteroidetes species.

*Diversity of N-cycling genes.* The temporal phylogenetic profile of each gene of interest was examined to elucidate the richness and diversity of genes comprising the nitrification and denitrification processes. Metagenomic reads containing sequence from the genes of interest were extracted from the total data set and assembled to yield partial and full-length gene

sequences (**Supplementary Data 1**). Phylogeny was determined for each assembled sequence, and phylotypes were defined at 90% amino acid sequence identity, since that level of similarity is typical between organisms of the same genus (Konstantinidis and Tiedje 2005). Richness was quantified for each gene as the number of distinct phylotypes identified. It was expected that detectable gene diversity would be considerably lower than organismal diversity, since 1) these activities are encoded by a subset of organisms, and 2) the assembly protocol is less sensitive than amplicon analysis, and thus only genes from abundant organisms are likely to be detected. Temporal diversity dynamics (turnover) were assessed by calculating the mean variance of relative abundance for phylotypes across time, and using a cumulative inverse Simpson calculation to examine species gain/loss (**Fig 3**).

Distinct diversity and turnover patterns were observed for each gene. The *narG* and *nosZ* genes, encoding the nitrate reductase large subunit and nitrous oxide reductase, respectively, had higher phylotype richness than the other nitrogen cycle genes examined (for *nosZ* vs *norB*, Welch's t-test p-value=0.0014, df=13.587), and their phylotype profiles had equivalent stability (Levene test p-value=0.1277) (**Fig 3, Fig S1A and Fig S2A**). While *nirK*/*nirS* (distinct types of nitrite reductase) and *norB* (nitric oxide reductase) had lower richness, their phylotype profile variability was significantly higher than for *narG* (Levene test p-values=0.00003, 0.0001, respectively), and were near significance for *nosZ* (Levene test p-values=0.0113, 0.0609 for *nosZ*I and *nosZ*II) (**Fig 3, Fig S3A and Fig S4A**). Both genes encoding activities involved in nitrification had extremely low phylotype diversity, *amoA* (ammonia oxidase) with 2 phylotypes, one bacterial and one archaeal, and *nxrA* (nitrite oxidase alpha subunit) having 7 observed, but one overwhelmingly dominant phylotype (**Fig S5A**). The low richness for *amoA* exaggerates the

phylotype abundance variance values, thus we consider the low richness to be the significant aspect of the *amoA* gene.

Community dynamics appeared to largely recycle a fixed pool of taxa. A cumulative diversity (inverse Simpson) plot showed all genes except *nosZ* plateauing or declining, indicating that the establishment of novel organisms with these genes into the community is rare (**Fig 4**). Seasonal effects were also observed. The *amoA* phylotype content was stable early and variable late, while *narG*, *norB*, and *nirKS* showed the reciprocal pattern, and *nxrA* showed no change in the level of variability.

*Abundance of N-cycling genes.* To assess temporal changes in the overall abundances of genes involved in denitrification and nitrification, the sets of all (*i.e.*, unassembled) metagenomic reads containing sequence from the genes of interest were enumerated, and the representation of each gene within the community was normalized across samples using counts of the conserved, single-copy *rplB* gene as a proxy for number of individuals sampled. Although gene abundances were relatively constant over time, the average abundances differed widely between genes. The *narG* gene, the first step in denitrification, was observed to be in 25-30% of the population, while *nirK/nirS* was represented in 35-45% of the population, and *norB* in 14-18% (**Fig 5A**). Nitrous oxide reductase genes (*nosZ*) were present in ~25% of the populations, however it is of note that the dominant form was *nosZ*II (also referred to in the literature as the 'atypical *nosZ*'), a distinct family of nitrous oxide reductases typically found in non-denitrifying organisms (Graf et al. 2014; Jones et al. 2014; Sanford et al. 2012). Nitrification genes showed more of a seasonal shift in abundance. The *amoA* gene, summing both the bacterial and archaeal versions, showed a low constant abundance of ~5% in early time points, and increased up near 30% late in the year

158 (**Fig 5B**). Unexpectedly, *nxrA* showed little correlation with *amoA*, displaying a trend of gradual
159 increase, ranging from 5% to 18%, early, and constancy late.
160
161 *Environmental drivers.* Regression analysis was performed to determine which, if any, of the
162 environmental parameters measured was associated with changes in diversity for the genes of
163 interest. Water temperature, dissolved oxygen (DO), dissolved organic carbon (measured as non-
164 purgeable organic carbon, NPOC), and chloride ($Cl^-$) measurements were used. $Cl^-$ is a
165 conservative indicator of the ratio of surface- to groundwater content in the hyporheic zone of
166 the study system (Stegen et al. 2018). Other measured constituents, $NO_3^-$ and $SO_4^-$ had strong
167 positive correlations with $Cl^-$ (**Fig S6**). Correlations between diversity (inverse Simpson),
168 richness, and abundance were tested against the environmental parameters. The strongest
169 relationships were with groundwater content (using $Cl^-$ as a proxy), with denitrification genes
170 *narG* ($R^2$=0.38; p=0.04) and *nosZ* ($R^2$=0.50; p=0.02) increasing in diversity (**Fig S7**),
171 nitrification genes *amoA* ($R^2$=0.41; p=0.03) and *nxrA* ($R^2$=0.44; p=0.03) increasing in abundance
172 (**Fig S8**), and *narG* ($R^2$=0.47; p=0.02) decreasing in abundance. Groundwater showed weaker
173 correspondence with increasing richness of *nxrA* ($R^2$=0.29; p=0.09), decreasing richness of
174 *nirKS* ($R^2$=0.27; p=0.10) (**Fig S9**), and decreasing abundance of *norB* ($R^2$=0.35; p=0.06). NPOC
175 had strongest correlations with the nitrification genes, showing a negative relationship with *nxrA*
176 diversity ($R^2$=0.31; p=0.08), and a positive relationship with *nirKS* richness ($R^2$=0.39; p=0.04)
177 and *narG* abundance ($R^2$=0.30; p=0.08). Temperature had a significant negative relationship
178 with *nxrA* diversity ($R^2$=0.33; p=0.08) and richness ($R^2$=0.45; p=0.03).
179
180 **DISCUSSION**

Shade *et al.*, in their review of microbial resistance and resilience, suggest that there is "no 'one-size fits all' response of microbial diversity and function to disturbance." (Shade et al. 2012). While this perspective is undoubtedly true, it leaves open the possibility that there are general patterns or rules that govern particular subsets or components of microbial communities. Here we begin to look for such patterns at a deeper level than previously examined by exploring dynamics in gene abundance and diversity within important biogeochemical processes in response to seasonal environmental changes. Building from recent work showing that component steps in biogeochemical processes are encoded by separate microbial taxa (Anantharaman et al. 2016; Mobberley et al. 2017), we hypothesized that within-gene diversity varies between component steps, and further that temporal dynamics of diversity would vary between steps. Our metagenomic data from a dynamic groundwater-surface water mixing zone were consistent with this hypothesis and demonstrated that within-gene diversity and the dynamics of that diversity are variable across genes. This outcome suggests that a community's taxonomic diversity or the abundance or diversity of any single (proxy) gene is not be a reliable predictor of stability in functional potential for multi-step biogeochemical processes, and that portions of the community that encode component steps with low within-gene diversity may be the most critical when considering potential decreases in function. Therefore, there is a need to shift the focus of analyses from taxonomic diversity or 'representative' gene abundances to a comprehensive understanding of within-gene diversity and dynamics across processes. Below we place these discoveries in context of previous work and point toward how they can be used to improve predictive models of system function.

*Diversity dynamics of nitrification genes.* The nitrification process showed low diversity at the two steps examined (**Fig 6**), leading to the possibility that these activities are susceptible to loss

or suppressed function. Nitrification was originally described as a cooperative process, requiring an ammonia oxidizing organism that produces nitrite and a nitrite oxidizing organism that converts the nitrite to nitrate (Winogradsky 1890). Recently, organisms have been identified that have both activities (comammox) (Daims et al. 2015). The range of organisms known to encode nitrification activities is narrow, although it does include both Bacteria (Nitrosomonas and Nitrospira) and Archaea (Thaumarchchaeota). The observed abundance of nitrifying organisms in sediment communities, both freshwater and marine, suggests nitrification is an important activity in the subsurface environment (Lansdown et al. 2014; Stoliker et al. 2016; Wang et al. 2012). The limited taxonomic distribution of nitrification activities in the hyporheic community was expected, however the low diversity, one phylotype for *nxrA*, and one sequence apiece for the bacterial and archaeal *amoA*s (Fig S5A and S5B) is extreme. This lack of diversity suggests these activities could be unstable, given observations demonstrating that community-level functional stability increases with diversity (Allison and Martiny 2008; Girvan et al. 2005; Tilman et al. 1997). However, we observed very stable abundance of these organisms across the seasonal shift in water chemistry, suggesting that the organisms encoding these activities are well adapted to the range of environmental conditions historically experienced by this community. Any extraordinary shift in biotic (*e.g.*, viruses, predation) or abiotic (*e.g.*, redox potential, temperature) conditions that selects against the small number of taxa involved in nitrification, however, could quickly degrade the community's nitrification potential. With no other apparent organisms available to supplement or take over this role, this fundamental service could be degraded or lost from this community, with unknown repercussions for the microbial community and the larger ecosystem (Dobson et al. 2006; Worm et al. 2006). Recently, nitrifiers, and in particular Archaeal nitrifiers, have been shown to be active in carbon fixation in freshwater

benthic sediments (Orsi 2018). Thus loss of nitrifiers could impact coupled carbon-nitrogen cycling in the subsurface and associated river corridors.

*Diversity dynamics of denitrification genes.* Denitrification genes have been identified in a broad range of taxa (Shapleigh 2013), and as such, our expectation was that within the hyporheic zone community there would be a high diversity across all component steps (Graham et al. 2016c; Schimel 1995). While we did observe considerable overall abundance of all genes, the levels of richness for the genes representing the individual activities varied, ranging from 52 phylotypes for nitrate reduction (*narG*) to 23 phylotypes for nitrite reductase (*nirK* and *nirS*) (**Fig 6**). This observation supports the concept that denitrification genes are distributed among members of the community as partial pathways or individual genes (Bru et al. 2011; Keil et al. 2011). Further, there was a surprising distribution of nitrous oxide reductase genes, with the type II form (*nosZ*II), which is typically found in non-denitrifying organisms (Sanford et al. 2012), having much greater abundance and richness (49 phylotypes) than the type I form (*nosZ*I, 2 phylotypes). Temporal variance of within-gene diversity for genes involved in both nitrification and denitrification demonstrates that the organisms encoding these activities are sensitive to different ecological selection pressures and thus different strategies are required to maintain functional potential in response to perturbation. For genes with high phylotype richness, high temporal abundance variance indicates a changing phylotype profile (*nirKS*, *norB*). These functions may be maintained through resilient microbial taxa that recover rapidly from environmental change. Conversely, low temporal variance (*narG*, *nosZ*) indicates a stable phylotype profile. These functions are maintained through resistant taxa that persist across a broad range of environmental conditions, with the possibility that the other low abundance phylotypes are capable of supplanting them should they fail under different conditions.

It is notable that while all genes associated with denitrification had high phylotype richness (in contrast to nitrification genes), the genes associated with intermediate reactions had higher temporal diversity variance than *narG* (Fig 2), which encodes the initial step in denitrification (i.e., nitrate reduction). One explanation for the observed differences could be that there are different levels of competition for the substrates fueling each activity. Intermediate substrates nitrite and nitric oxide may be produced slowly and/or consumed quickly, especially considering there are multiple cellular processes for which they are intermediates and they are both toxic to cells. Supporting this contention, nitrite is typically undetectable in samples from this location, while nitrate is readily detectable (Graham et al. 2017). Low availability would lead to high substrate competition, which could result in the increased phylotype turnover observed in *nirK*, *nirS* and *norB* genes. Modeling the redundancy provided to a process by within-gene diversity thus requires an understanding of temporal variation in the selective pressures for each gene involved.

*Influence of seasonal changes in hydrogeochemsitry.* Seasonal changes in groundwater to surface water ratios appear to be a major influence on N-cycling functional potential in microbial communities. Increase in groundwater content corresponded to increasing per-capita abundance of nitrification genes and decreasing abundance/increasing diversity of denitrification genes. The *nirKS* and *norB* gene families, which displayed similar high phylotype turnover behavior, were not similar in their response to the environmental parameters measured, with *nirKS* showing a decrease in richness in response to groundwater while *norB* showed a decrease in abundance. The *narG* and *nosZ* gene families, which showed more stable profiles, both increased in diversity in response to groundwater, however, *nosZ* did so through increased richness, while *narG* likely gained evenness through reduced abundance of dominant phylotypes. Organic carbon (NPOC)

had a much weaker association with gene-level metrics, relative to groundwater. A group of co-occurring organisms with a negative correlation to groundwater has been reported in this sediment system (Graham et al. 2017). The group is dominated by Alpha-, Beta- and Gammaproteobacteria, Bacteroidetes and Planctomycetes, the same taxa that encode nearly all of the identified denitrification genes. Strong homogenous selection was shown to be the mechanism structuring this group (Graham et al. 2016a). Taken together, these data suggest that some factor other than carbon that is within the groundwater is the selective force driving the diversity dynamics of these organisms carrying N-cycling genes. A likely candidate is the N content of groundwater, which is significantly higher than that of the surface water (Stegen et al. 2018).

*Gene diversity and process resilience.* Conceptualizing and studying diversity within individual gene families is a departure from the contemporary perspective that largely focuses on organismal diversity or abundances of gene families. Variation in diversity across component steps of key biogeochemical processes and the dynamics of within-gene diversity in response to environmental change is therefore unexplored. This hampers our ability to predict ecosystem responses to future environmental changes. To illustrate the importance of diversity across individual component steps of biogeochemical processes, we use the analogy of an electrical circuit (**Fig 7**). Continuity from one step to the next is required for the full process/circuit to function. To preserve integrity of the circuit there is parallelization within each component step, whereby there are multiple options for completing a given step (Condition A). In a biological context, this manifests as multiple organisms encoding the same activity through different alleles of the same gene. Under different environmental conditions, various options may not be available either because the conditions are not favorable to the expression or operation of the

gene, or the organism encoding that gene is eliminated from the community. The function is maintained by the availability or introduction of alternates that can function under the new conditions (Condition B). Conditions may exist, however, under which no options for a given component step are available to the system, for example if an anaerobic system was exposed to sufficient oxygen to inhibit nitrous oxide reductase activity. This scenario will prevent the full biogeochemical process (e.g., denitrification) from completing, at least temporarily, even if the some component steps are functioning (Condition C). Steps with low within-gene diversity are more likely to experience environmental conditions that cause all options to be eliminated. Just as a chain is only as strong as its weakest link, the ability of a metabolic pathway to continue functioning is determined by the component step with the lowest diversity.

We propose that accounting for the influence of environmental variation on realized biogeochemical rates in predictive models should connect environmental conditions to the dynamics of component steps. Doing so would allow models to account for variation in the susceptibility of each step to perturbation, based on within-gene diversity and dynamics. For example, reaction network models could represent the combined influence of gene-level abundance and diversity on continued function during and after perturbation. Recent modeling developments open up such opportunities, such as Song et al.'s reaction network model that explicitly represents control of enzyme expression at each step along a given biogeochemical pathway (Song et al. 2017). This model could be easily modified to represent different levels of diversity and abundance of gene phylotypes across component steps. Numerical experiments using the resulting model could comprehensively explore the sensitivity of biogeochemical function to among-step variation in within-gene diversity and dynamics. We also contend that there is a need to incorporate within-gene diversity into our conceptualization of diversity and

focus on understanding the ecological processes governing diversity within individual genes. Merging such ecological knowledge with mechanistic biogeochemical models should improve our ability to predict biogeochemical function under future environmental conditions.

## Experimental Procedures

*Sampling.* Sediment communities were captured using sand packs incubated within piezometers as described (Graham et al. 2016a). Briefly, 1.2 m, fully-screened, stainless steel piezometers (5.25 cm inner diameter) were deployed along the margin of the Columbia River at approximately 46° 22' 15.80"N, 119° 16' 31.52"W. Sand packs composed of ~80 $cm^3$ of locally-sourced medium grade sand (>0.425mm <1.7mm) packed into 2 x 4.5", 18/8 mesh stainless steel infuser plugged with Pyrex fiber glass were sterilized by combustion at 450°C for 8hr and then deployed in pairs for six week incubations collected at three week intervals from April 30, 2014 to November 25, 2014. Upon retrieval, paired sand packs were combined and homogenized. A ~145 mL subsample was flash-frozen and transported on dry ice back to the laboratory for metagenomic analysis. Aqueous samples were taken as previously described (Graham et al. 2016a). Briefly, at each piezometer, peristaltic pumps and manifolds were purged for 10-15 minutes. Following the purge, water was pumped through 0.22 µm polyethersulfone Sterivex filters for 30 minutes. Filtered water was used for water chemistry analysis.

*Water Chemistry.* Water chemistry was determined as previously described (Graham et al. 2016a). Briefly, water temperature was measured with a handheld meter (Ultrameter II, Myron L Co Carlsbad, CA). A YSI Pro ODO handheld with an optical DO probe (YSI Inc. Yellow Springs, OH) was used to measure dissolved oxygen. NPOC was determined by the combustion

342 catalytic oxidation/NDIR method using a Shimadzu TOC-Vcsh with ASI-V auto sampler
343 (Shimadzu Scientific Instruments, Columbia, MD). Samples were acidified with 2 N HCl and
344 sparged for 5 minutes to remove DIC. The sample was then injected into the furnace set to
345 680$^{o}$C. Nitrate concentrations were determined on a Dionex ICS-2000 anion chromatograph with
346 AS40 auto sampler. A 25-minute gradient method was used with a 25-µL injection volume and a
347 1 mL/min flow rate at 30$^{o}$C (EPA-NERL: 300.0).
348
349 *DNA extraction.* Genomic DNA was prepared from sediment samples as previously described
350 (Graham et al. 2016a). Briefly, to release biomass, thawed samples were suspended in 20mL of
351 chilled PBS /0.1% Na-pyrophosphate solution and vortexed for 1 min. The suspended fraction
352 was decanted to a fresh tube and centrifuged for 15' at 7000 x g at 10$^{o}$C. DNA was extracted
353 from the resulting pellets using the MoBio PowerSoil kit in plate format (MoBio Laboratories,
354 Inc., Carlsbad, CA) following manufacturer's instructions with the addition of a 2 hour
355 proteinase-K incubation at 55$^{o}$C prior to bead-beating to facilitate cell lysis.
356
357 *Sequencing.* Genomic DNA purified from sandpack samples was submitted to the Joint Genome
358 Institute under JGI/EMSL proposal 1781 for paired-end sequencing on an Illumina HiSeq 2500
359 sequencer. Results from the sequencing are presented in **Table S1**. Data sets are available
360 through the JGI Genome Portal (http://genome.jgi.doe.gov). Project identifiers are listed in Table
361 S1.
362
363 *Metagenomic analysis.* To quantitate gene families of interest, hidden Markov models (HMMs)
364 were obtained or built and searched against raw metagenomic reads. HMMs used in this study

are listed in **Table 1**. HMMs were searched against raw reads using MaxRebo (Lee Ann McCue, unpubl.), which translates each read in six frames, and searches the translations against the target HMM(s), using HMMer (Eddy 2011) on a distributed, high-performance computing framework. Output was screened for reads with a significant score (e-value ≤ 1e-25) against the HMM. Raw counts were converted to RPKM (reads per kilobase of gene length per million reads) using the HMM length x 3 as the gene length. Results from forward and reverse reads were averaged and normalized against the summed RPKMs of the rplB and rplB_arch models. Individual genes of interest were assembled from the combined metagenomic datasets using the Xander assembler (Wang et al. 2015) and the HMMs listed in Table 1 and associated required files. Resulting contigs were clustered at 90% amino acid identity (**Supplementary Data 1**) to define phylotypes. Phylogeny was assessed by aligning protein sequences with mafft v7.164b (Katoh et al. 2002; Katoh and Standley 2013) and constructing approximated maximum-likelihood trees using FastTree v2.1.9 (Price et al. 2010). Phylotype profiles were determined by searching individual metagenomic read sets against the resulting gene contigs and calculating RPKM values and normalizing against the summed phylotype RPKM for the gene. Bray-Curtis dissimilarity between samples for each gene was calculated using the R package vegan (Dixon 2003), and resulting values were used to generate a boxplot.

*Community analysis.* Amplicon data used was from Graham et al., 2016b. Bray-Curtis distance was determined as described below, and plotted using R.

*Statistics.* Bray-Curtis dissimilarity, as implemented in the R package vegan (Dixon 2003), was used to measure beta diversity. Values were averaged for both the total dataset and the T4 dataset

388 alone. Early (n=6) versus late (n=5) gene abundance comparisons were tested for significance
389 using the Mann-Whitney-Wilcoxon test as implemented in R v.3.3.2 (https://www.r-project.org).
390 For turnover heatmaps, assembled sequences were searched against the read set to estimate
391 individual abundances. Sequences were then clustered into phylotypes at 90% identity, and
392 abundances summed. The relative abundance of each phylotype was then determined by dividing
393 its abundance by the summed abundance of all phylotypes of the gene in question. Trees were
394 determined from nucleic acid sequence alignments (mafft) using the maximum-likelihood
395 approach implemented in FastTree. Inverse Simpson statistic for the assembled sequences was
396 calculated cumulatively for each gene at each time point, also using the vegan package. Linear
397 regressions and associated $R^2$ and p-values were calculated in R v3.3.2.
398
399 **Acknowledgments**
400 This research was supported by the US Department of Energy (DOE), Office of Biological and
401 environmental Research (BER), as part of Subsurface Biogeochemical Research Program's
402 Scientific Focus Area (SFA) at the Pacific Northwest National Laboratory (PNNL). PNNL is
403 operated for DOE by Battelle under contract DE-AC06-76RLO 1830. A portion of the research
404 was performed using Institutional Computing at PNNL. Sequencing was done at the DOE Joint
405 Genome Institute under Community Science Project 1781.
406
407 **Conflict of Interest**
408 The authors declare no conflicts of interest, financial or otherwise, regarding the design,
409 execution or reporting of this study.
410

411 **Table 1. HMMs used in this study**

| Gene | HMM | Source |
|---|---|---|
| **Nitrate reductase, alpha subunit (narG)** | narG | FunGene[1] |
| **Cu-containing nitrite reductase (nirK)** | | |
| **Clade I** | nirK1 | PNNL[2] |
| **Clade II** | nirK2 | PNNL |
| **Fe-containing nitrite reductase (nirS)** | nirS | FunGene |
| **Nitric oxide reductase (norB)** | | |
| **Copper** | norB_cNor | FunGene |
| **quinone** | norB_qNor | FunGene |
| **Nitrous oxide reductase** | | |
| **nosZI** | nosZ | FunGene |
| **'non-denitrifying' (nosZII)** | nosZ_a2 | FunGene |
| **Ammonia monooxygenase** | | |
| **bacterial** | amoA_AOB | FunGene |
| **archaeal** | amoA_AOA | FunGene |
| **Nitrite oxidoreductase, alpha subunit** | nxrA-1 | PNNL |
| **Ribosomal protein RplB** | | |
| **bacterial** | rplB | FunGene |
| **archaeal** | rplB_arch | PNNL |

412 [1] Available at https://github.com/rdpstaff/Xander_assembler

413 [2] Available at https://github.com/wichne/Xander_files

414

## Figure legends

**Figure 1. Water chemistry and temperature of sampled sites.** Piezometer T2, light gray; piezometer T3, dark gray; piezometer T4, black. For comparison, data for adjacent river water is presented (blue). The vertical dotted line indicates the date at which the hyporeheic zone hydraulic regime changes from surface water intrusion to groundwater discharge.

**Figure 2. Sediment microbial community continuously changes across the year.** Distance-decay plot of all 16S rRNA amplicon data, amplicon data from only site T4, and *rplB* genes assembled from all metagenomes.

**Figure 3. Relationship between phylotype richness and turnover.** Unique sequences assembled from the metagenomic dataset were clustered into phylotypes using a 90% amino acid identity cutoff.

**Figure 4. Change in cumulative diversity over time.** Inverse Simpson was calculated cumulatively for each time point for each gene or functional gene class (*nirK* and *nirS* counts were combined; archaeal and bacterial *amoA* types were combined) and the difference from the initial (April 30) diversity measure determined. Most genes' values plateau, indicating sample-to-sample changes in diversity are within a finite pool of phylotypes. Increase indicates introduction of new phylotypes, or increases in evenness. Decrease for *amoA* is driven by a decrease in evenness between the bacterial and archaeal phylotypes (Fig S5A), whereas the early decrease for *nirKS* was driven largely by species loss (Fig S3A).

**Figure 5. Per-capita abundance of denitrification and nitrification genes.** RPKM for each gene was normalized against the RPKM for the *rplB* gene as a proxy for the number of individuals sampled. **A** Denitrification genes. **B** Nitrification genes.

**Figure 6. Redundancy diagram of nitrification and denitrification activities.** Individual lines represent phylotypes. Colors represent different HMMs used to identify genes of each family: for AmoA, blue=amoA_AOA, red=amoA_AOB; for NirKS, red=nirK1, blue=nirK2, green=nirS; for NorB, yellow=qNorB, blue=cNorB; for NosZ, magenta=nosZI, green=nosZ_a2; NxrA and NarG each only had one model.

**Figure 7. Circuit diagram of a metabolic pathway.** Steps in series convert substrates (S), to various intermediates (I1, I2), to a product (P). Redundancy is represented by parallel paths, which can be regulated individually (denoted by arrow gates). Under conditions A and B, product is produced, but by different paths, whereas under condition C, although the blue and green steps are active, neither of the orange steps are, preventing production of I2 and P.

# REFERENCES

Allison, S. D., and J. B. Martiny. 2008. Colloquium paper: resistance, resilience, and redundancy in microbial communities. Proc Natl Acad Sci U S A **105 Suppl 1:** 11512-11519.

Anantharaman, K. and others 2016. Thousands of microbial genomes shed light on interconnected biogeochemical processes in an aquifer system. Nat Commun **7:** 13219.

Bru, D. and others 2011. Determinants of the distribution of nitrogen-cycling microbial communities at the landscape scale. ISME J **5:** 532-542.

Daims, H. and others 2015. Complete nitrification by Nitrospira bacteria. Nature **528:** 504-509.

Dixon, P. 2003. VEGAN, a package of R functions for community ecology. J Veg Sci **14:** 927-930.

Dobson, A. and others 2006. Habitat loss, trophic collapse, and the decline of ecosystem services. Ecology **87:** 1915-1924.

Eddy, S. R. 2011. Accelerated Profile HMM Searches. PLoS Comput Biol **7:** e1002195.

Gibbons, S. M., and J. A. Gilbert. 2015. Microbial diversity--exploration of natural ecosystems and microbiomes. Curr Opin Genet Dev **35:** 66-72.

Girvan, M. S., C. D. Campbell, K. Killham, J. I. Prosser, and L. A. Glover. 2005. Bacterial diversity promotes community stability and functional resilience after perturbation. Environ Microbiol **7:** 301-313.

Graf, D. R. H., C. M. Jones, and S. Hallin. 2014. Intergenomic Comparisons Highlight Modularity of the Denitrification Pathway and Underpin the Importance of Community Structure for N2O Emissions. Plos One **9**.

Graham, E. B. and others 2016a. Coupling Spatiotemporal Community Assembly Processes to Changes in Microbial Metabolism. Frontiers in Microbiology **7**.

---. 2016b. Coupling Spatiotemporal Community Assembly Processes to Changes in Microbial Metabolism. Front Microbiol.

Graham, E. B. and others 2017. Deterministic influences exceed dispersal effects on hydrologically-connected microbiomes. Environ Microbiol **19:** 1552-1567.

Graham, E. B. and others 2016c. Microbes as Engines of Ecosystem Function: When Does Community Structure Enhance Predictions of Ecosystem Processes? Front Microbiol **7:** 214.

Graham, E. B. and others 2014. Do we need to understand microbial communities to predict ecosystem function? A comparison of statistical models of nitrogen cycling processes. Soil Biol Biochem **68:** 279-282.

Hooper, D. U. and others 2005. Effects of biodiversity on ecosystem functioning: A consensus of current knowledge. Ecol Monogr **75:** 3-35.

Jones, C. M. and others 2014. Recently identified microbial guild mediates soil N2O sink capacity. Nat Clim Change **4:** 801-805.

Katoh, K., K. Misawa, K. Kuma, and T. Miyata. 2002. MAFFT: a novel method for rapid multiple sequence alignment based on fast Fourier transform. Nucleic Acids Res **30:** 3059-3066.

Katoh, K., and D. M. Standley. 2013. MAFFT multiple sequence alignment software version 7: improvements in performance and usability. Mol Biol Evol **30:** 772-780.

Keil, D. and others 2011. Influence of land-use intensity on the spatial distribution of N-cycling microorganisms in grassland soils. Fems Microbiol Ecol **77:** 95-106.

Konstantinidis, K. T., and J. M. Tiedje. 2005. Genomic insights that advance the species definition for prokaryotes. Proc Natl Acad Sci U S A **102:** 2567-2572.

Lansdown, K. and others 2014. Fine-Scale in Situ Measurement of Riverbed Nitrate Production and Consumption in an Armored Permeable Riverbed. Environ Sci Technol **48:** 4425-4434.

Mobberley, J. M. and others 2017. Organismal and spatial partitioning of energy and macronutrient transformations within a hypersaline mat. Fems Microbiol Ecol **93**.

493 Nelson, M. B., R. Berlemont, A. C. Martiny, and J. B. Martiny. 2015. Nitrogen Cycling Potential of a
494 Grassland Litter Microbial Community. Appl Environ Microbiol **81:** 7012-7022.
495 Nelson, M. B., A. C. Martiny, and J. B. Martiny. 2016. Global biogeography of microbial nitrogen-cycling
496 traits in soil. Proc Natl Acad Sci U S A **113:** 8033-8040.
497 Price, M. N., P. S. Dehal, and A. P. Arkin. 2010. FastTree 2--approximately maximum-likelihood trees for
498 large alignments. PLoS One **5:** e9490.
499 Rosenfeld, J. S. 2002. Functional redundancy in ecology and conservation. Oikos **98:** 156-162.
500 Sanford, R. A. and others 2012. Unexpected nondenitrifier nitrous oxide reductase gene diversity and
501 abundance in soils. Proc Natl Acad Sci U S A **109:** 19709-19714.
502 Schimel, J. 1995. Ecosystem Consequences of Microbial Diversity and Community Structure. Ecol Stu An
503 **113:** 239-254.
504 Shade, A. and others 2012. Fundamentals of microbial community resistance and resilience. Frontiers in
505 Microbiology **3**.
506 Shapleigh, J. P. 2013. Denitrifying Prokaryotes, p. 405-425. *In* E. Rosenberg, E. F. DeLong, S. Lory, E.
507 Stackebrandt and F. Thompson [eds.], The Prokaryotes: Prokaryotic Physiology and
508 Biochemistry. Springer Berlin Heidelberg.
509 Song, H. S., N. Goldberg, A. Mahajan, and D. Ramkrishna. 2017. Sequential computation of elementary
510 modes and minimal cut sets in genome-scale metabolic networks using alternate integer linear
511 programming. Bioinformatics **33:** 2345-2353.
512 Stegen, J. C. and others 2018. Influences of organic carbon speciation on hyporheic corridor
513 biogeochemistry and microbial ecology. Nat Commun **9:** 585.
514 Stoliker, D. L. and others 2016. Hydrologic Controls on Nitrogen Cycling Processes and Functional Gene
515 Abundance in Sediments of a Groundwater Flow-Through Lake. Environ Sci Technol **50:** 3649-
516 3657.

517 Tilman, D., J. Knops, D. Wedin, P. Reich, M. Ritchie, and E. Siemann. 1997. The influence of functional
518 diversity and composition on ecosystem processes. Science **277:** 1300-1302.
519 Torsvik, V., and L. Ovreas. 2002. Microbial diversity and function in soil: from genes to ecosystems. Curr
520 Opin Microbiol **5:** 240-245.
521 Walker, B. H. 1992. Biodiversity and Ecological Redundancy. Conserv Biol **6:** 18-23.
522 Wang, Q. and others 2015. Xander: employing a novel method for efficient gene-targeted metagenomic
523 assembly. Microbiome **3:** 32.
524 Wang, Z. Y., Y. Qi, J. Wang, and Y. S. Pei. 2012. Characteristics of aerobic and anaerobic ammonium-
525 oxidizing bacteria in the hyporheic zone of a contaminated river. World J Microb Biot **28:** 2801-
526 2811.
527 West, S. A., and G. A. Cooper. 2016. Division of labour in microorganisms: an evolutionary perspective.
528 Nature Reviews Microbiology **14:** 716.
529 Winogradsky, S. 1890. Recherches sur les organismes de la nitrification. Ann. Inst. Pasteur **4:** 213-231.
530 Worm, B. and others 2006. Impacts of biodiversity loss on ocean ecosystem services. Science **314:** 787-
531 790.
532 Yachi, S., and M. Loreau. 1999. Biodiversity and ecosystem productivity in a fluctuating environment:
533 The insurance hypothesis. P Natl Acad Sci USA **96:** 1463-1468.
534 Zumft, W. G. 1997. Cell biology and molecular basis of denitrification. Microbiol Mol Biol Rev **61:** 533-
535 616.

536

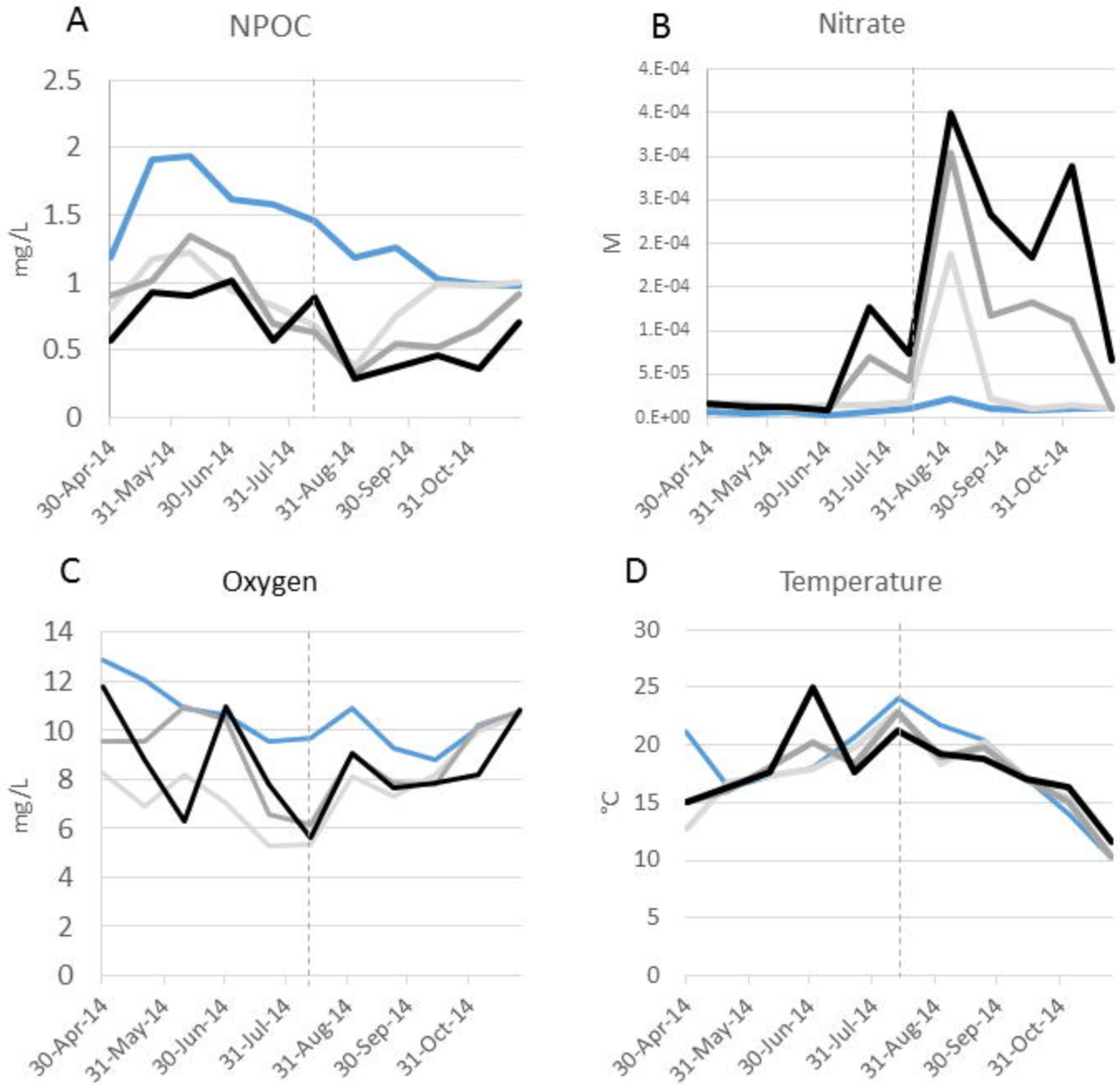
A
NPOC
mg/L
2.5
2
1.5
1
0.5
0
30-Apr-14
31-May-14
30-Jun-14
31-Jul-14
31-Aug-14
30-Sep-14
31-Oct-14
B
Nitrate
M
4.E-04
4.E-04
3.E-04
3.E-04
2.E-04
2.E-04
1.E-04
5.E-05
0.E+00
C
Oxygen
mg/L
14
12
10
8
6
4
2
0
D
Temperature
°C
30
25
20
15
10
5
0

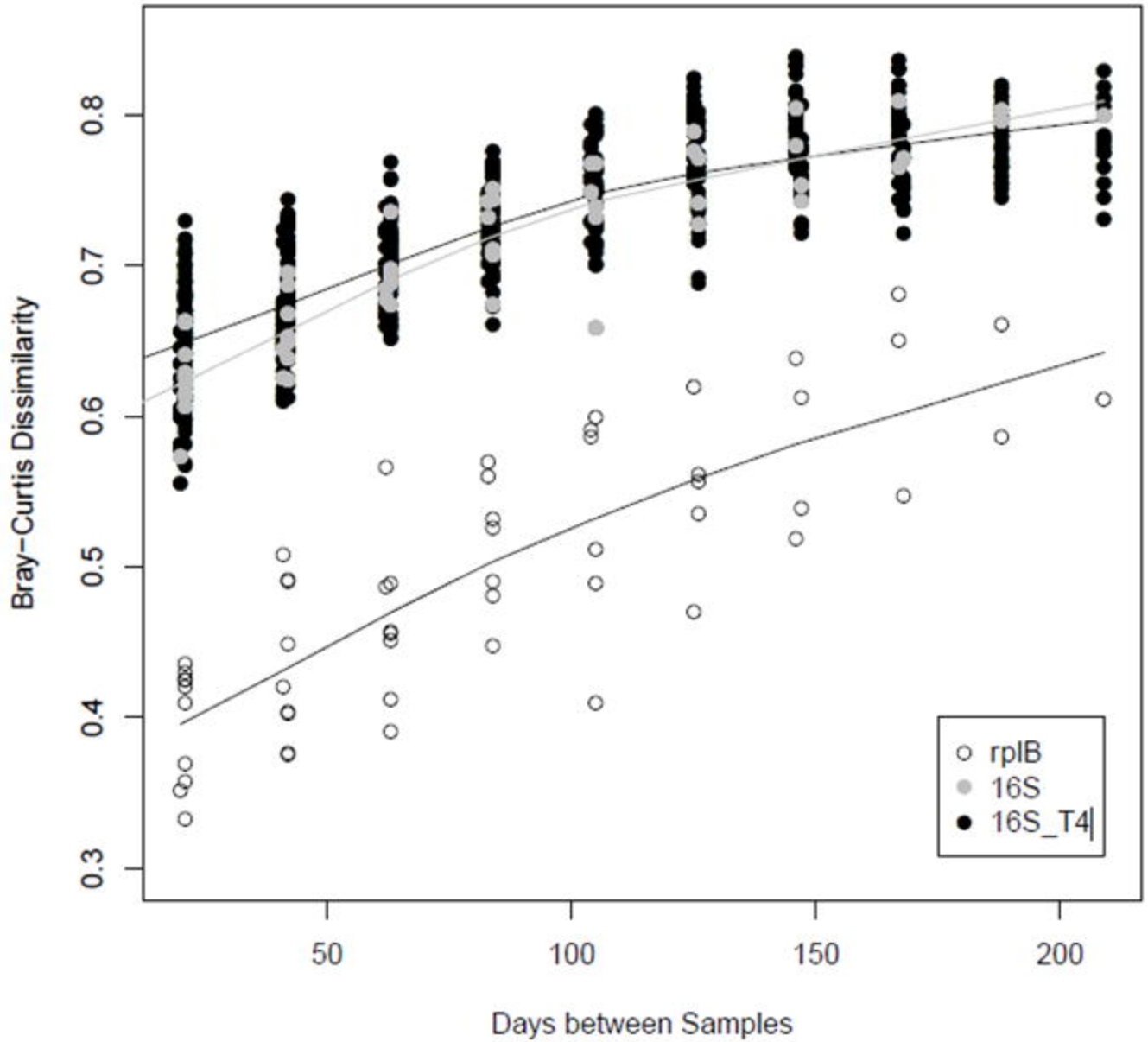
Bray−Curtis Dissimilarity
0.3
0.4
0.5
0.6
0.7
0.8
50
100
150
200
Days between Samples
rplB
16S
16S_T4

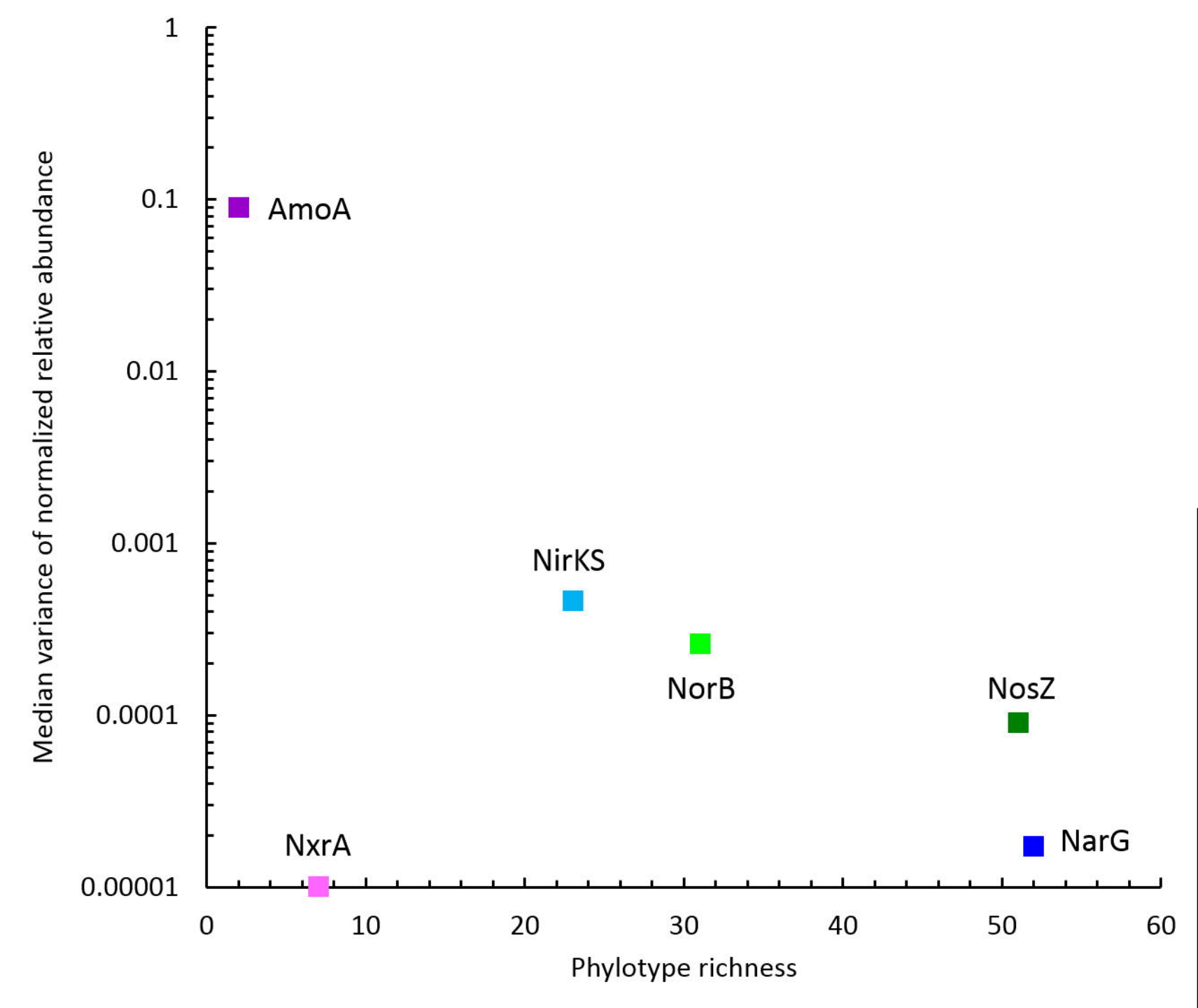
1
0.1
0.01
0.001
0.0001
0.00001
Median variance of normalized relative abundance
AmoA
NirKS
NorB
NosZ
NxrA
NarG
0
10
20
30
40
50
60
Phylotype richness

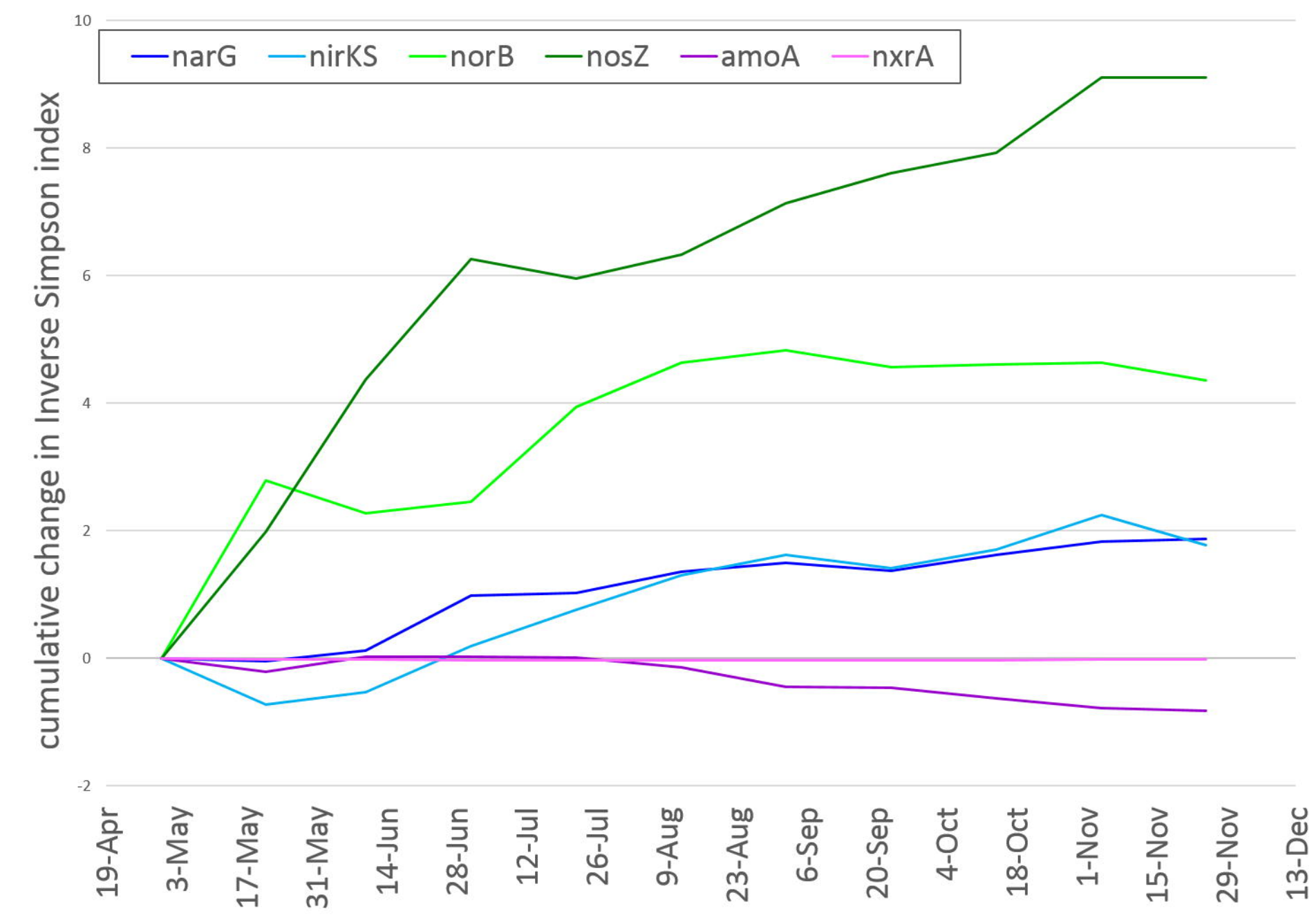
narG
nirKS
norB
nosZ
amoA
nxrA
cumulative change in Inverse Simpson index
10
8
6
4
2
0
-2
19-Apr
3-May
17-May
31-May
14-Jun
28-Jun
12-Jul
26-Jul
9-Aug
23-Aug
6-Sep
20-Sep
4-Oct
18-Oct
1-Nov
15-Nov
29-Nov
13-Dec

a

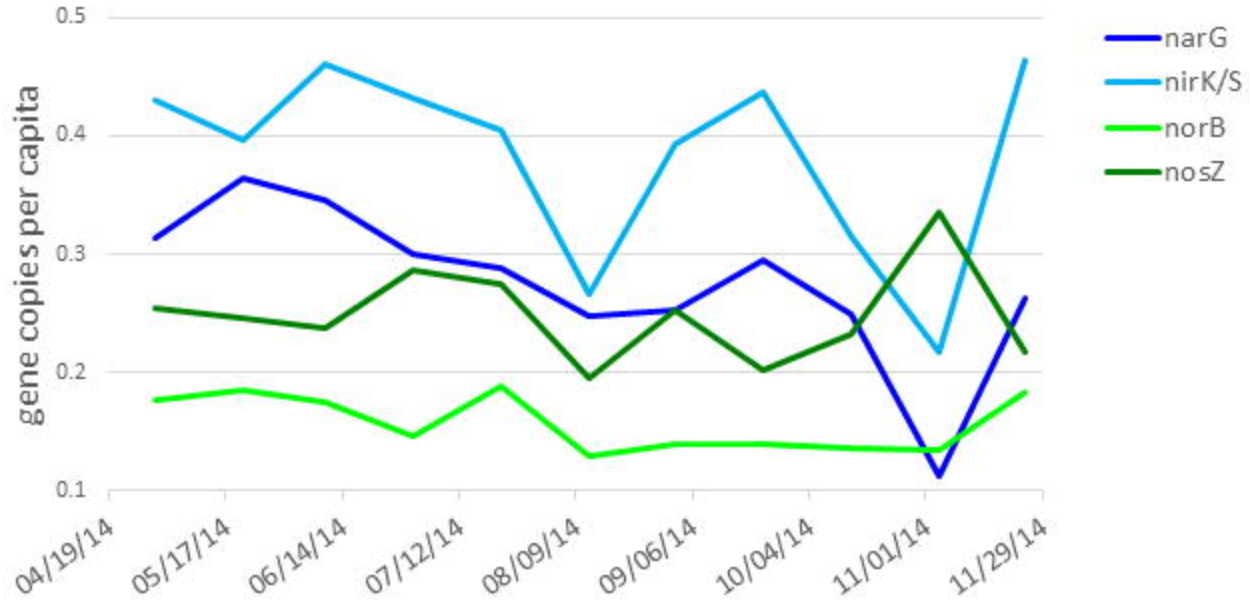
0.5
0.4
0.3
0.2
0.1
gene copies per capita
04/19/14
05/17/14
06/14/14
07/12/14
08/09/14
09/06/14
10/04/14
11/01/14
11/29/14
narG
nirK/S
norB
nosZ

b

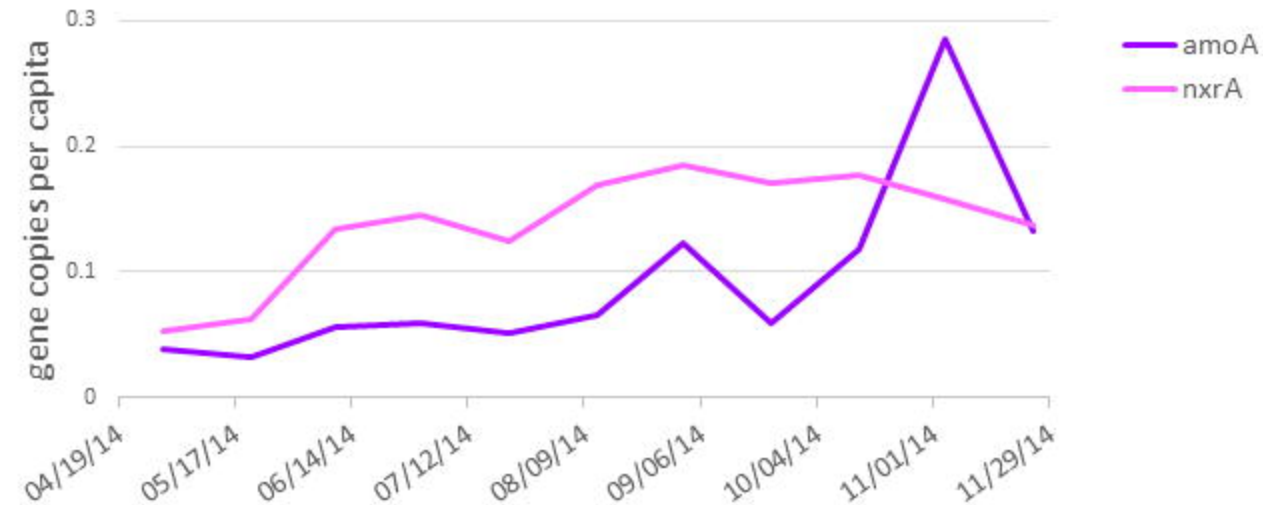
0.3
0.2
0.1
0
gene copies per capita
04/19/14
05/17/14
06/14/14
07/12/14
08/09/14
09/06/14
10/04/14
11/01/14
11/29/14
amoA
nxrA

## Nitrification

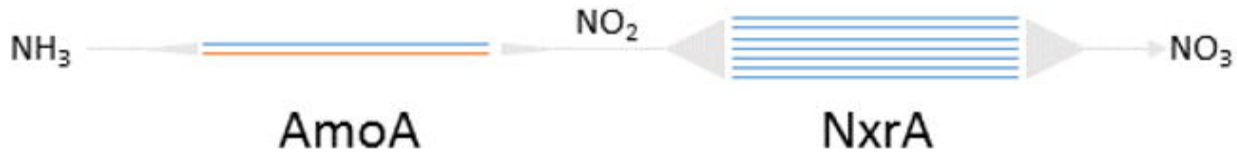


## Denitrification

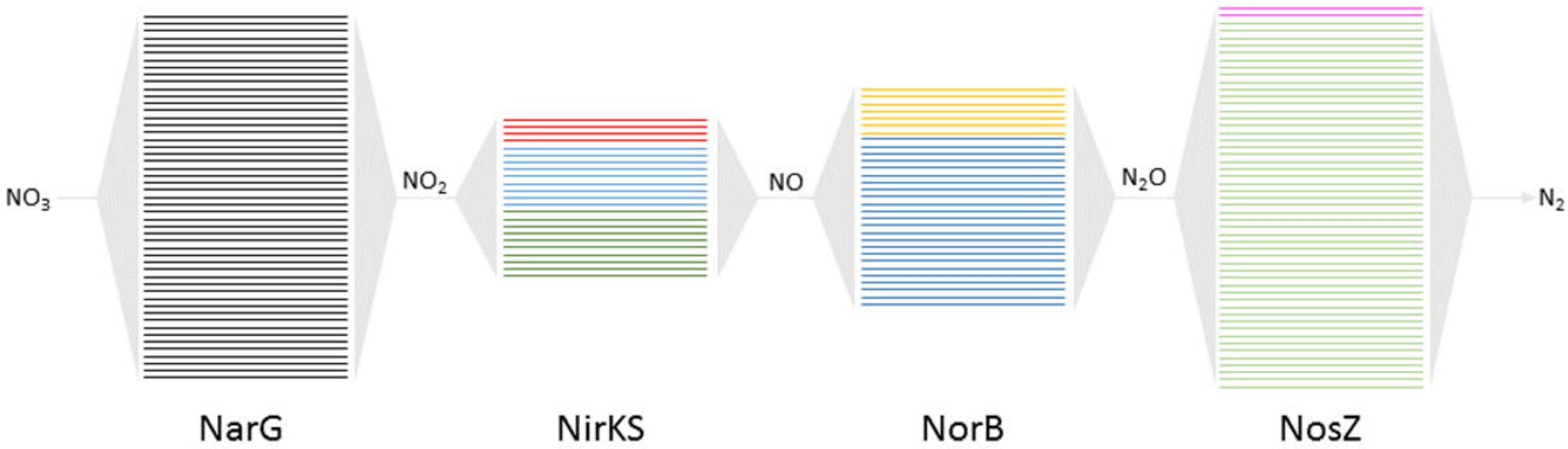

Condition A

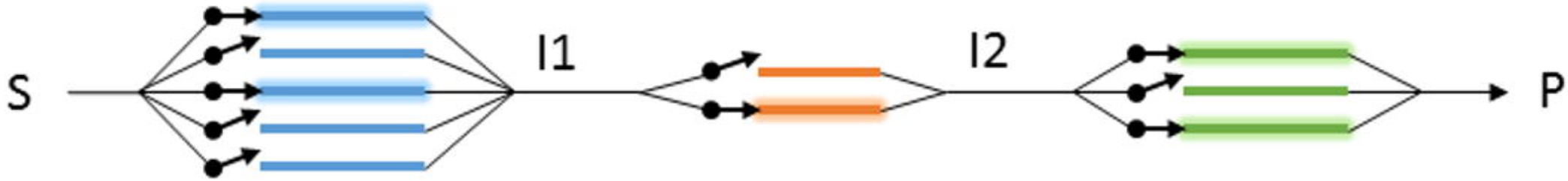


Condition B

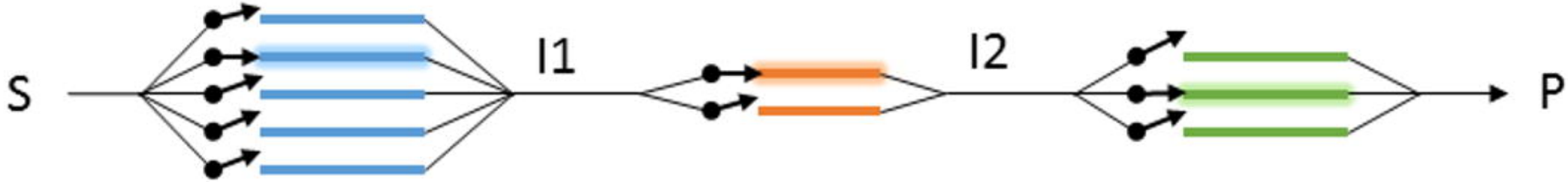


Condition C